Modeling, Simulation, and Kinetic Analysis of a Heterogeneous Reaction System for the Enzymatic Conversion of Poorly Soluble Substrate

Dong-Cheol Lee,* Joo-Ho Park, Geun-Joong Kim, Hak-Sung Kim

Department of Biological Sciences, Korea Advanced Institute of Science and Technology, 373-1, Kusung-Dong, Yusung-Gu, Taejon 305-701, Korea; telephone: +82-42-869-2616; fax: +82-42-869-2610; e-mail: +hskim@sorak.kaist.ac.kr

Received 17 July 1998; accepted 23 December 1998

Abstract: We developed a kinetic model that describes a heterogeneous reaction system consisting of a solid substrate suspension for the production of D-amino acid using D-hydantoinase. As a biocatalyst, mass-produced free and whole cell enzymes were used. The heterogeneous reaction system involves dissolution of a solid substrate, enzymatic conversion of the dissolved D-form substrate, spontaneous racemization of an L-form substrate to D-form, and deactivation of the enzyme. In the case of using whole cell enzymes, transfer of the dissolved substrate and product through the cell membrane was considered. The kinetic parameters were determined from experiments, literature data, and by using Marquardt's method of nonlinear regression analysis. The model was simulated using the kinetic parameters and compared with experimental data, and a good agreement was observed between the experimental results and the simulation ones. Factors affecting the kinetics of the heterogeneous reaction system were analyzed on the basis of the kinetic model, and the efficiency of the reaction systems using free and whole cell enzymes was also compared. © 1999 John Wiley & Sons, Inc. *Biotechnol Bioeng* **64**: 272–283, 1999.

Keywords: D-hydantoinase; heterogeneous reaction system; kinetic model; substrate suspension; D-amino acid

INTRODUCTION

Optically active D-amino acids find wide applications as building blocks of semisynthetic antibiotics, insecticides, and sweetners and are currently produced from 5-substituted hydantoins using microbial D-hydantoinase (Syldatk et al., 1990; Yamada et al., 1978). In the D-hydantoinase-catalyzed process, a racemic mixture of chemically synthesized D,L-5-mono-substituted hydantoin is used as a starting substrate. Of the two isomers, D-form substrate is asymmetrically hydrolyzed to *N*-carbamoyl-D-amino acid by D-hydantoinase, and this intermediate is further converted to the corresponding D-amino acid either by a chemical method or by an enzymatic one using D-carbamoylase (Ogawa et al., 1994; Runser et al., 1990). The unreacted L-form substrate is spontaneously racemized to the D-form under alkaline conditions, and, theoretically, a 100% conversion yield is obtained.

In an effort to develop the D-hydantoinase-catalyzed process for the production of D-amino acids, we isolated the D-hydantoinase form *Bacillus stearothermophilus* SD-1 (Lee et al., 1995) and cloned and overexpressed the gene encoding the enzyme in *Escherichia coli* (Lee et al., 1996). For the practical application, the enzyme was successfully mass-produced by batch culture of recombinant *E. coli* (Lee et al., 1997). Among various D-amino acids, we focused on D-*p*-hydroxyphenylglycine since this D-amino acid has the large commercial demand. In this case, a racemic mixture of chemically synthesized D,L-5-(4-hydroxyphenyl)hydantoin (HPH) was used as the starting substrate.

In the development of the enzymatic process, however, the low solubility of the substrate HPH has been a serious problem. The solubility of HPH in water is reported to be about 60–70 m*M* (Takahashi, 1986). To overcome the solubility problem, we tried using various organic solvents, but no positive effect was observed in terms of the reaction rate and conversion yield in the D-hydantoinase-catalyzed reaction. As an alternative approach, we carried out the enzyme reaction in a heterogeneous reaction system in which most of the substrate is present in suspended particles and optimized the reaction system (Lee and Kim, 1998). So far, the heterogeneous reaction system consisting of solid substrate has been attempted in steroid biotransformation (Constantinides, 1980; Maxon et al., 1966), and the hydantoinase-catalyzed reaction with moderate substrate concentration (Deepa et al., 1993; Lee and Lin, 1996; Olivieri et al., 1981), but systematic analyses on the kinetics of the reaction system have not been performed. Recently, a kinetic model was tested for α-chymotrypsin-catalyzed hydrolysis of benzylmethylmalonate (Wolff et al., 1997), and in this case, deactivation of the enzyme was not considered, and a very low concentration of solid substrate (~2 g/L) was used.

Present address: Pacific Corporation/R&D Center, 314-1, Borari, Kiheung-eup, Kongin-si, Kyounggi-do 449-900 Korea

Correspondence to: H.-S. Kim

CCC 0006-3592/99/030272-12

In order to better understand the kinetics of the heterogeneous reaction system and to optimize it for practical application, a detailed kinetic analysis of the reaction system is a prerequisite.

In this paper, we present the kinetic model which describes the heterogeneous reaction system for the production of *N*-carbamoyl-D-*p*-hydroxyphenylglycine (NCHPG), which is readily converted to D-*p*-hydroxyphenylglycine under acidic conditions, from poorly soluble 5-(4-hydroxyphenyl)hydantoin (HPH) by using the mass-produced D-hydantoinase. The model involves dissolution of the solid substrate, enzymatic conversion of the D-form substrate, racemization of the L-form substrate to the D-form, and deactivation of the enzyme. In the case of the whole cell enzyme, transfer of the dissolved substrate and product through the cell membrane was considered. The performance of the reaction systems using free and whole cell enzymes was predicted and compared with the experimental results (Lee and Kim, 1998). Factors affecting the kinetics of the heterogeneous reaction systems were also analyzed on the basis of the kinetic model.

MODEL DEVELOPMENT

In order to develop a kinetic model which describes the heterogeneous reaction system, the reaction system was firstly analyzed in more detail. Fig. 1 shows the schematic diagram of the reaction systems using free and whole cell enzymes. In the case of the free enzyme system (Fig. 1A), the solid substrate (HPH) dissolves into the reaction mixture, and of the two enantiomers, the dissolved D-form substrate is hydrolyzed to N-carbamoyl-D-p-hydroxyphenylglycine (NCHPG) by the enzyme. As the enzymatic reaction proceeds, unreacted L-form substrate is spontaneously racemized to D-form. Production of NCHPG results in the pH drop of the reaction mixture, and NaOH solution is added for titration. The enzyme is subject to deactivation by several factors during the reaction. When the whole cell enzyme is used (Fig. 1B), the system is almost the same as the free enzyme system except that there is a transport barrier for the substrate and product across the cell membrane because the enzymes are inside the cell membrane. As a result, the transfer rates of solubilized substrate and product are affected by their permeabilities through the cell membrane. The enzyme inside the cells also loses its activity during the reaction.

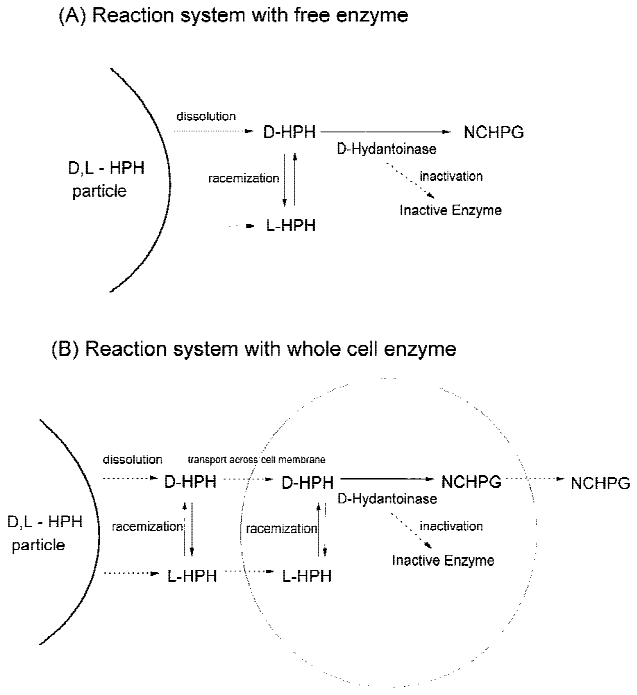

Figure 1. Schematic diagrams of the heterogeneous reaction systems using free (A) and whole cell enzymes (B).

On the basis of the above analysis, we established a mathematical model of the heterogeneous reaction system for the conversion of poorly soluble substrate using free and whole cell enzymes.

Free Enzyme System

The dissolution rate of solid substrate can be expressed as

$$\frac{dS}{dt} = k_s a_p (S^* - S). \tag{1}$$

The dissolution process is independent of the substrate chirality, and the k_s is assumed to be constant over the range of operating conditions. The size and shape of the substrate particles are presumed to be even and spherical.

Dissolution of solid substrate results in the reduction of particle size, and the change of particle radius, R, is given by the following equations:

$$\rho_H N_p \, 4\pi R^2 \left(-\frac{dR}{dt} \right) = k_s N_p 4\pi R^2 \, (S^* - S_D - S_L). \tag{2a}$$

Thus,

$$\frac{dR}{dt} = -\frac{k_s}{\rho_H} (S^* - S_D - S_L), \tag{2b}$$

where N_p is the number of substrate particles per unit volume of the aqueous phase.

Of the two isomers, dissolved D-form substrate is hydrolyzed to NCHPG by the enzyme, and the reaction rate is expressed by the simple Michaelis–Menten kinetic as

$$-\frac{dS_D}{dt} = \frac{k_{cat} E \, S_D}{K_m + S_D}. \tag{3}$$

As the enzymatic reaction proceeds, the concentration of D-form substrate decreases, and the spontaneous racemization of L-form substrate to D-form occurs. The racemization rate is described by first-order reversible reaction as

$$\frac{dS_D}{dt} = k_R (S_L - S_D), \tag{4}$$

where k_R is assumed to be constant under given reaction conditions.

Change in the concentrations of D- and L-form substrates in aqueous phase depends on the dissolution, enzymatic reaction, and racemization rates. From the material balance for each substrate, variation in the concentrations of D- and L-form substrates is given by

$$\frac{dS_D}{dt} = k_s N_p 2\pi R^2 (S^* - S_D - S_L) + k_R(S_L - S_D) - \frac{k_{cat} E S_D}{K_m + S_D}, \quad (5)$$

$$\frac{dS_L}{dt} = k_s N_p 2\pi R^2 (S^* - S_D - S_L) + k_R (S_D - S_L). \quad (6)$$

All the concentrations in the equations are calculated with respect to the volume of aqueous phase, V_{aq}, where the volume of substrate particles is excluded. During the reaction, NaOH solution is added for titration, leading to an increase in the volume of the aqueous phase. Thus, the volume of added NaOH solution was included in the volume of the aqueous phase. The effect of evaporation of the reaction mixture and the soluble product on the volume of the aqueous phase was assumed to be negligible. Production rate of NCHPG based on the volume of aqueous phase is calculated as

$$\frac{dP}{dt} = \frac{k_{cat} E S_D}{K_m + S_D}. \quad (7)$$

As for the deactivation of the enzyme, there might be several factors which cause the deactivation. In this work, we made a hypothesis that the enzyme loses its activity by spontaneous deactivation, by the presence of solid substrate particles, and by NaOH added for titration based on the previous experimental results (Lee and Kim, 1998). Spontaneous deactivation of the enzyme is assumed to follow the first-order kinetics, and the deactivation rate is expressed by

$$-\frac{dE}{dt} = k_d E. \quad (8)$$

The mechanism by which the enzyme is deactivated by the presence of solid substrate particles is not clearly demonstrated, but surface tension on the interface between the solid and aqueous phases might be the main contributing factor. The effect of solid substrate particles on the activity of D-hydantoinase was previously predicted by using invertase instead of D-hydantoinase because it was difficult to determine the D-hydantoinase activity during the reaction. Deactivation of invertase became more serious with the increasing concentration of HPH particles (Lee and Kim, 1998). On the basis of this observation, we assumed that the deactivation rate of the enzyme by the substrate particles is proportional to the enzyme concentration and the interfacial area between the solid and aqueous phases. Consequently, deactivation rate is expressed as

$$-\frac{dE}{dt} = k_p a_p E. \quad (9)$$

Effect of NaOH on the deactivation of the enzyme was also investigated. Figure 2 shows the stability of the whole cell enzyme at different loadings when the substrate concentration was 300 g/L. Deactivation of the enzyme was more serious with increasing enzyme loading at a given substrate concentration. In other words, as the enzyme loading increases, the addition rate of NaOH also increases due to the enhanced production rate of NCHPG, which leads to more rapid deactivation of the enzyme. Deactivation of the enzyme by NaOH added for titration seems to occur during mixing time. From this result, deactivation of the enzyme by NaOH was presumed to be proportional to the addition rate of NaOH as follows.

$$-\frac{dE}{dt} = k_{NaOH} E \gamma_{NaOH}, \quad (10)$$

where γ_{NaOH} is the addition rate of NaOH solution. Consequently, time-course variation in the active enzyme concentration is given by

$$\frac{dE}{dt} = -k_{d,aq} E - k_p N_p 4\pi R^2 E - \frac{k_{NaOH,aq}}{1 + 4/3 N_p \pi_L R^3} \frac{k_{cat} E S_D}{k_m + S_D} E, \quad (11)$$

where all the concentrations are also expressed with respect to V_{aq}

Whole Cell Enzyme System

In the case of using whole cell enzyme as a biocatalyst, two points are different from the free enzyme system (Fig. 1B). One is that there is a transport barrier for the substrate and product across the cell membrane since the enzymes are inside the cell membrane, and consequently, the production rate of NCHPG is affected by the transfer rates of the sub-

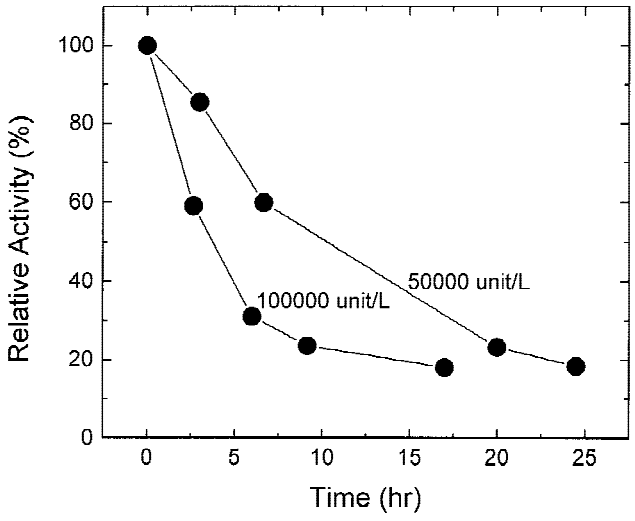

Figure 2. Time course of activity of whole cell enzyme at different loadings of the whole cell enzyme when the substrate concentration was 300 g/L. Temperature and pH of the reaction were maintained at 45°C and 8.5.

strate and product across the cell membrane. The other is that deactivation of the enzyme by the presence of substrate particles is negligible because the enzymes are inside the cell membrane. Dissolution of solid substrate, enzymatic conversion of D-form substrate, and racemization of L-form substrate are the same as those in the free enzyme system, and accordingly the change in the particle size is expressed the same way as in the Eq. (2b).

Transfer rates of dissolved substrate and product are assumed to be proportional to their permeability through the cell membrane and the surface area of the cells. Therefore, the transfer rate of dissolved D-form substrate is expressed by

$$-\frac{dS_D}{dt} = h_S A_C (S_D - S_{D,C}). \tag{12}$$

As for the L-form substrate, a similar equation is obtained.

The permeability of substrate and product might be affected by the extent of permeabilization of the cell membrane. Change in the activity of the whole cell enzyme was determined in a buffer solution at 45°C as a function of incubation time. As shown in Fig. 3, the apparent specific activity of the whole cell enzyme increased with incubation time, probably due to the permeabilization of the cell membrane. On the basis of this experimental result, a saturation model was employed to describe the change in the permeabilities of the substrate and product through the cell membrane. For the substrate, the permeability, h_s, is expressed as a function of reaction time by

$$h_S = h_{S,0} + (h_{S,max} - h_{S,0}) \frac{t}{P_m + t}. \tag{13}$$

The permeability of product, h_p, was assumed to be related with that for the substrate by a constant ratio, α, over the reaction time (see section Parameter Evaluation), and becomes

$$h_p = \alpha h_S. \tag{14}$$

From the mass balance, variations in the concentrations of dissolved D- and L-form substrates in the aqueous phase are given by

$$\frac{dS_D}{dt} = k_S N_p 2\pi R^2 (S^* - S_D - S_L) + k_R (S_L - S_D) - h_S A_C (S_D - S_{D,C}), \tag{15}$$

$$\frac{dS_L}{dt} = k_S N_p 2\pi R^2 (S^* - S_D - S_L) + k_R (S_D - S_L) - h_S A_C (S_L - S_{L,C}), \tag{16}$$

where the concentrations are expressed with respect to V_{aq} except for $S_{D,C}$ and $S_{L,C}$, which are based on the total cell volume V_C.

Change in the concentration of substrate inside the cells is influenced by the transfer rate of dissolved substrate into the cells and the enzymatic reaction rate. The conversion rate of D-form substrate to the product obeys the Michelis–Menten kinetics as the free enzyme system. The mass balances for each substrate inside the cells are

$$\frac{dS_{D,C}}{dt} V_C = h_S A_C (S_D - S_{D,C}) V_{aq} + k_R (S_{L,C} - S_{D,C}) V_C - \frac{k_{cat} E_C S_{D,C}}{K_m + S_{D,C}} V_C \tag{17a}$$

$$\frac{dS_{L,C}}{dt} V_C = h_S A_C (S_L - S_{L,C}) V_{aq} + k_R (S_{D,C} - S_{L,C}) V_C \tag{18a}$$

Thus, the time course of the change in the concentrations of D- and L-form substrates inside the cells can be written as

$$\frac{dS_{D,C}}{dt} = h_S A_C (S_D - S_{D,C}) \frac{V_{aq}}{V_C} + k_R (S_{L,C} - S_{D,C}) - \frac{k_{cat} E_C S_{D,C}}{K_m + S_{D,C}}, \tag{17b}$$

$$\frac{dS_{L,C}}{dt} = h_S A_C (S_L - S_{L,C}) \frac{V_{aq}}{V_C} + k_R (S_{D,C} - S_{L,C}). \tag{18b}$$

The concentrations are calculated with respect to the toal cell volume, V_C, in the reaction mixture except for S_D, S_L, and A_C which are based on V_{aq}.

By a similar procedure, the mass balances for the product inside the cells and in the aqueous phase are established as below.

$$\frac{dP_C}{dt} V_C = \frac{k_{cat} E_C S_{D,C}}{K_m + S_{D,C}} V_C - h_p A_C (P_C - P) V_{aq}, \tag{19a}$$

$$\frac{dP}{dt} V_{aq} = h_p A_C (P_C - P) V_{aq}. \tag{20a}$$

Arrangement of the above equations yields

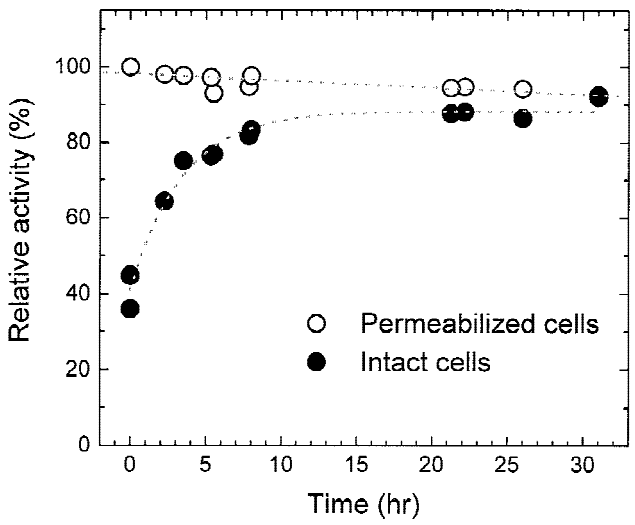

Figure 3. Change in the specific activity of whole cell enzyme with incubation time in 0.01 *M* Tris-HCl buffer (pH 8.5). Temperature was 45°C.

Table I. Kinetic parameter values used in the simulation of the model.

Estimation method	Parameter	Value	Dimension
Experiments	k_{cat}	5.5×10	s^{-}
	K_m	2.3×10^{-2}	mol/L
	$k_{d,aq}$	7.6×10^{-6}	s^{-1}
	$k_{d,C}$	7.1×10^{-7}	s^{-1}
	ρ_H	7.8	mol/L
	S^*	7.0×10^{-2}	mol/L
Marquardt's method of nonlinear regression analysis	k_p	$(3.8 \pm 0.2) \times 10^{-6}$	cm/s
	$k_{NaOH,aq}$	1.8 ± 0.1	$(mol/L)^{-1}$
	$k_{NaOH,C}$	2.1 ± 0.02	$(mol/L)^{-1}$
	$h_{s,max}$	$(3.5 \pm 0.6) \times 10^{-6}$	cm/s
	$h_{s,0}$	$(3.5 \pm 1.5) \times 10^{-8}$	cm/s
	P_m	$(4.0 \pm 1.4) \times 10^3$ for 300 g/L substrate $(2.0 \pm 0.04) \times 10^4$ for 50 g/L substrate	s
Literature data	k_s	1.0×10^{-3}	cm/s
	k_R	1.2×10^{-3}	s^{-1}
	α	1.0×10^{-1}	—

$$\frac{dP_C}{dt} = \frac{k_{cat}E_C S_{D,C}}{K_m + S_{D,C}} - h_P A_C (P_C - P)\frac{V_{aq}}{V_C}, \quad (19b)$$

$$\frac{dP}{dt} = h_P A_C (P_C - P). \quad (20b)$$

The whole cell enzyme also loses its activity during the reaction as the free enzyme, but deactivation by substrate particles is assumed to be negligible because the enzymes exist inside the cells. In the case, the mass balance for the active enzyme inside the cells is

$$\frac{dE_C}{dt}V_C = -k_{d,C}E_C V_C - k_{NaOH,C}\frac{[k_{cat}E_C S_{D,C}/(K_m + S_{D,C})]V_C}{(1 + 4/3N_P\pi R^3)V_{aq}}E_C V_C. \quad (21a)$$

Thus, the deactivation rate of the enzyme is expressed by

$$\frac{dE_C}{dt} = -k_{d,C}E_C - \frac{k_{NaOH,C}}{1 + 4/3N_P\pi R^3}\frac{k_{cat}E_C S_{D,C}}{K_m + S_{D,C}}E_C\frac{V_C}{V_{aq}}. \quad (21b)$$

For the calculation of A_C and V_C, the shape of E. coli cells was assumed to be a round-ended rod with a dimension of 1.0 μm × 5.0 μm (Singleton and Sainsbury, 1987). Consequently, the volume and surface area of single E. coli cells were calculated to be about 3.7×10^{-18} m^3 and 1.6×10^{-11} m^2, respectively. Microscopic observations revealed no alteration in the shape of the cells during the reaction (Lee and Kim, 1998), and consequently the number of cells in the reaction mixture was presumed to remain constant.

MATERIALS AND METHODS

Experiments

Experimental conditions were the same as described elsewhere (Lee et al., 1997; Lee and Kim, 1998). The previously obtained data (Lee and Kim, 1998) were used in simulation and analysis of the kinetic model.

Parameter Evaluation

Kinetic parameters appearing in the model equations were determined by various methods, and are summarized in Table I. The k_{cat}, K_m, $k_{d,aq}$, and $k_{d,C}$ were determined from independent experiments. For the k_{cat} and K_m, initial reaction rates were obtained at different substrate concentrations below the solubility limit at pH 8.5 and 45°C, and a double-reciprocal plot was carried out. Since the enzyme has no activity toward the L-form substrate, the K_m for D-form HPH was estimated under the assumption that the concentration of D-form substrate is half that of a racemic mixture. For the estimation of the $k_{d,aq}$ and $k_{d,C}$, free and whole cell enzymes were incubated in the same condition, and the time

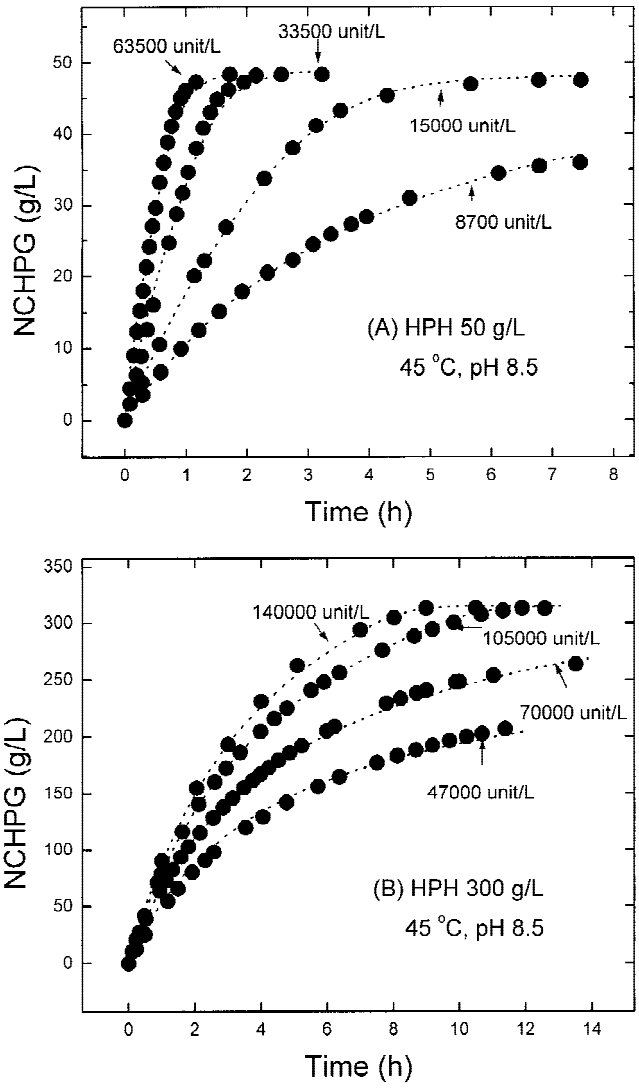

Figure 4. Profiles of product formation at different loadings of free enzyme. Substrate concentrations were (A) 50 g/L and (B) 300 g/L. Symbols indicate the experimental data, and dotted lines indicate simulation data.

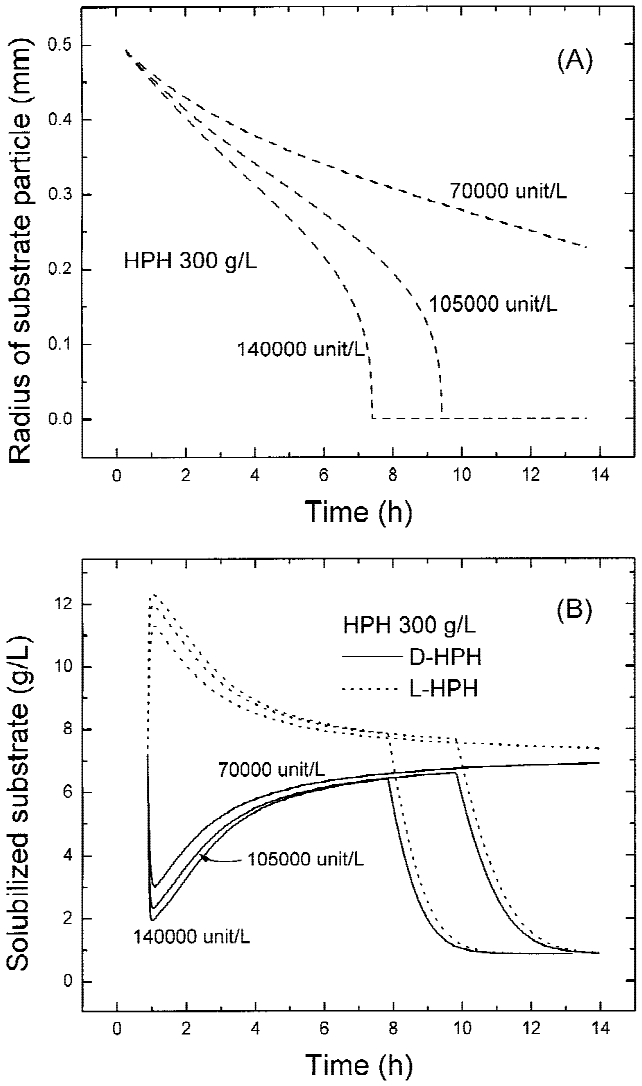

Figure 5. Predicted change in the size of substrate particles (A), and the concentrations of the dissolved D- and L-form substrates (B) for the reaction using free enzymes.

course of the change in the enzyme activity was traced. From the $k_{d,aq}$ and $k_{d,C}$, it was found that the free enzyme loses its activity ten times faster than the whole cell enzyme. The solubility of HPH, S^*, was determined in 0.1 *M* Tris-HCl buffer (pH 8.5) at 45°C by using a spectrophotometer according to the procedure reported elsewhere (Constantinides, 1980; Mall et al., 1995). The density of HPH, ρ_H, was estimated by the method described elsewhere (Shugar and Ballinger, 1996).

The mass transfer coefficient of HPH, k_s, was approximated from a simple correlation with critical suspension speed and Schmidt number (μ/PD) in a mechanically agitated tank as described elsewhere (Jadhav and Pangarkar, 1991). Racemization rate constant, k_R, was calculated from the experimental data of Cecere (1975). Information on the ratio of h_p to h_s, α, is not available, and experimental determination of α value was difficult. It was also impossible to confidently estimate the α value by using Marquardt's method of nonlinear regression analysis (see below) because the sensitivity of this value to the profiles of the product formation was very low (see Fig. 13D). In this work, the α value was assumed to be about 0.1 on the basis of the literature data (Tranchino and Melle, 1990).

The values of k_p and $k_{NaOH,aq}$ for the free enzyme, and $k_{NaOH,C}$, $h_{S,max}$, $h_{S,0}$, and P_m for the whole cell enzyme were simultaneously estimated by using Marquardt's method of nonlinear regression analysis. This numerical method is based on a linear combination of the steepest-descent and Gauss–Newton methods and is most commonly used to find a set of parameters satisfying the least-squares criterion (Constantinides, 1987; Johnson and Faunt, 1992). Profiles of product formation with reaction time were experimentally obtained for various substrate concentrations and enzyme loadings, and the kinetic parameters of the model which minimize the overall sum of squared residuals were

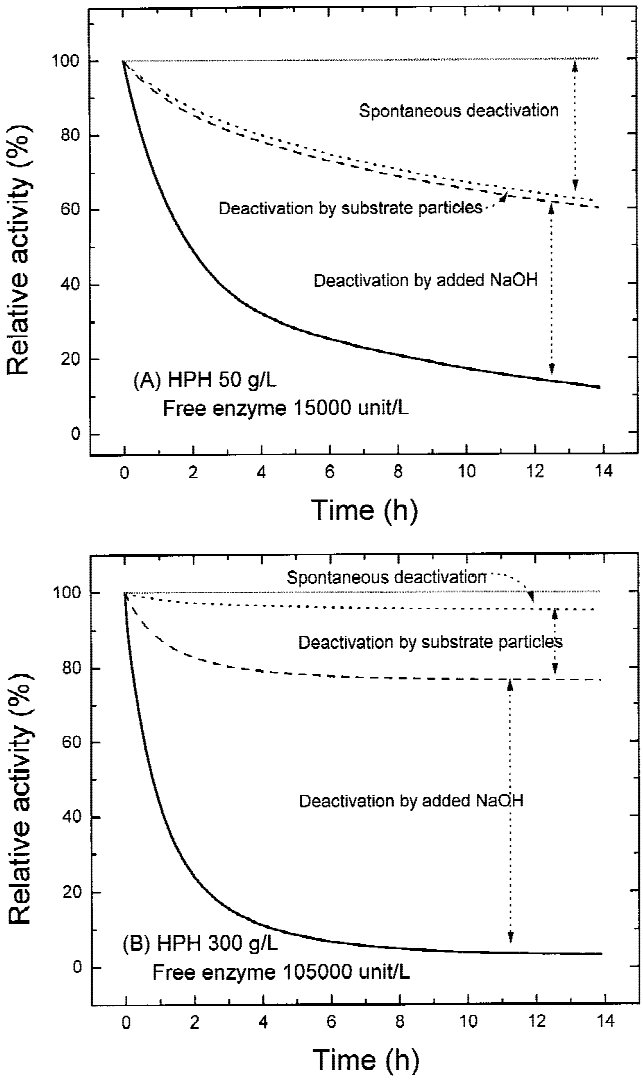

Figure 6. Predicted portion of each deactivation factor to total deactivation of the enzyme in the free enzyme system.

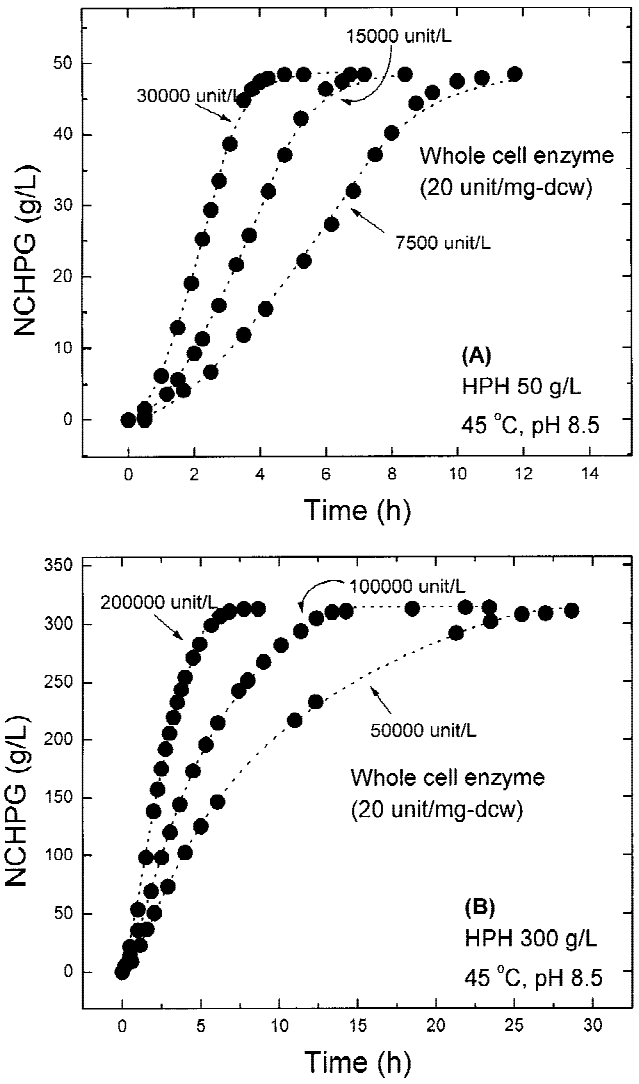

Figure 7. Profiles of product formation at different loadings of whole cell enzyme. Substrate concentrations were (A) 50 g/L and (B) 300 g/L. Symbols indicate the experimental data, and dotted lines indicate simulation data.

estimated by fitting the model to the experimental data. Production profiles obtained in the following conditions were used for the parameter estimation: 105,000 units/L of free enzyme and 300 g/L HPH; 50,000 units/L of whole cell enzyme and 300 g/L HPH; 7500 units/L of whole cell enzyme and 50 g/L HPH. The parameter values obtained from the experiments and literature data were used in determination of the kinetic parameters using the Marquardt's method of nonlinear regression analysis. The estimated parameter values were found to be equivalently reproducible for each data set within the region of 95% confidence intervals, except for the P_m value. The P_m value was calculated to be different with different substrate concentrations as expected. Previous experimental results revealed that the time required for the whole cell enzyme to be fully permeabilized decreases with increasing substrate concentration (Lee and Kim, 1998).

Solution of Model Equations

The model equations for the free and whole cell enzyme systems were numerically integrated using 4th-order Runge–Kutta method. The kinetic parameters summarized in Table I were used for integration. Nonlinear regression analyses by Marquardt's method and integration of model equations were performed using the BASIC programs described elsewhere with modifications (Constantinides, 1987). An IBM PC with a 586 microprocessor operating at 133 MHz was used.

RESULTS AND DISCUSSION

Simulation of Free Enzyme System

Figure 4 shows the profiles of product formation at different loadings of free enzymes when the substrate concentrations were 50 and 300 g/L. Symbols indicate the experimental results, and dotted lines indicate the simulation results. In each simulation, the same kinetic parameters shown in Table I were used, and good agreement was observed between the experimental results and the simulations. Increase in the volume of the reaction mixture due to the addition of NaOH solution was considered in the calculation of product concentration.

Change in particle size with reaction time is predicted in Fig. 5A when the initial particle size is assumed to be 0.5 mm. Particle size decreases more sharply with increasing enzyme loading, which indicates that dissolution rate concomitantly increases as the solubilized substrate is consumed more rapidly due to the enhanced enzyme reaction rate. Changes in the concentrations of the dissolved D- and L-form substrates are shown in Fig. 5B. The concentration of D-form substrate drops fast at the beginning of the reaction. On the other hand, in the case of L-form substrate, the

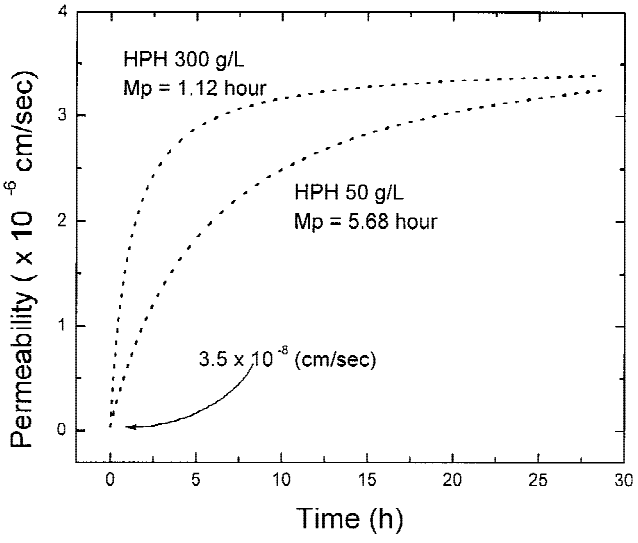

Figure 8. Predicted change in the permeability of substrate through the cell membrane with reaction time.

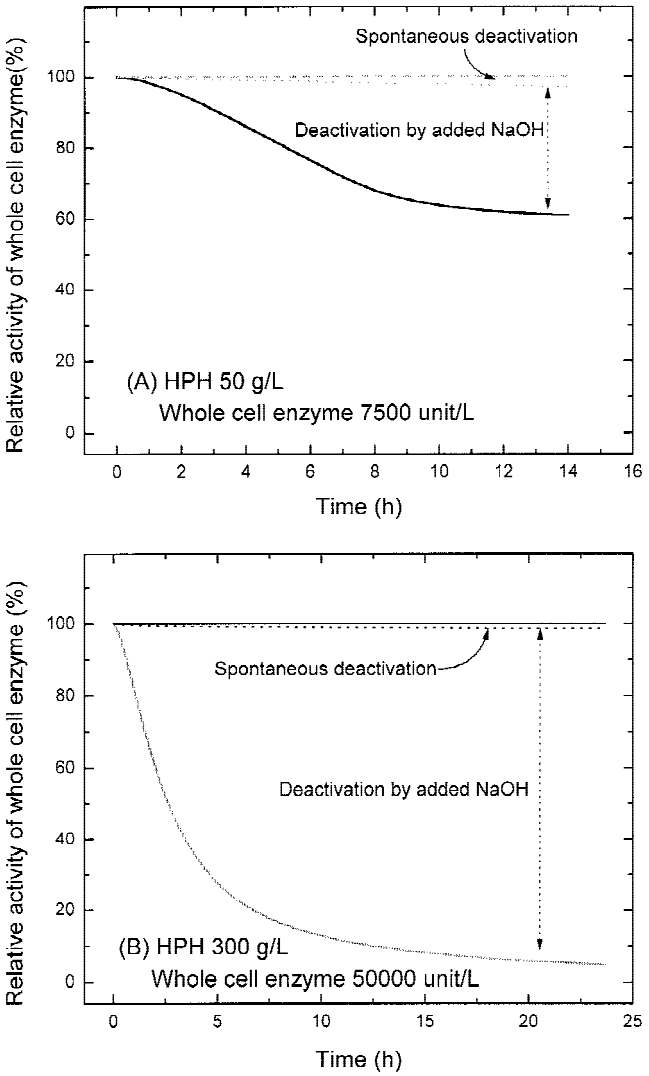

Figure 9. Predicted portion of each deactivation factor to total deactivation of the enzyme in the whole cell enzyme system.

concentration increases, showing a symmetrical pattern to that of D-form substrate, and the sum of the dissolved D- and L-form substrates maintains at its solubility in water. The rapid decrease in the concentration of D-form substrate at the beginning of the reaction is due to the fact that the consumption rate of D-form substrate is much higher than the racemization rate of L-form to D-form substrate. As the reaction proceeds, however, the concentration of D-form substrate gradually increases due to the reduced enzyme reaction rate caused by deactivation of the enzyme, resulting in a decrease in the L-form substrate. The concentrations of D- and L-form substrates drop to zero when there are no more particles in the reaction mixture.

As described in Model Development, the enzyme is presumed to lose its activity by spontaneous deactivation, substrate particles, and NaOH added for titration. Contribution of each factor to the total deactivation of the enzyme is predicted for different substrate concentrations. As shown in Fig. 6A and B, deactivation of the enzyme by NaOH

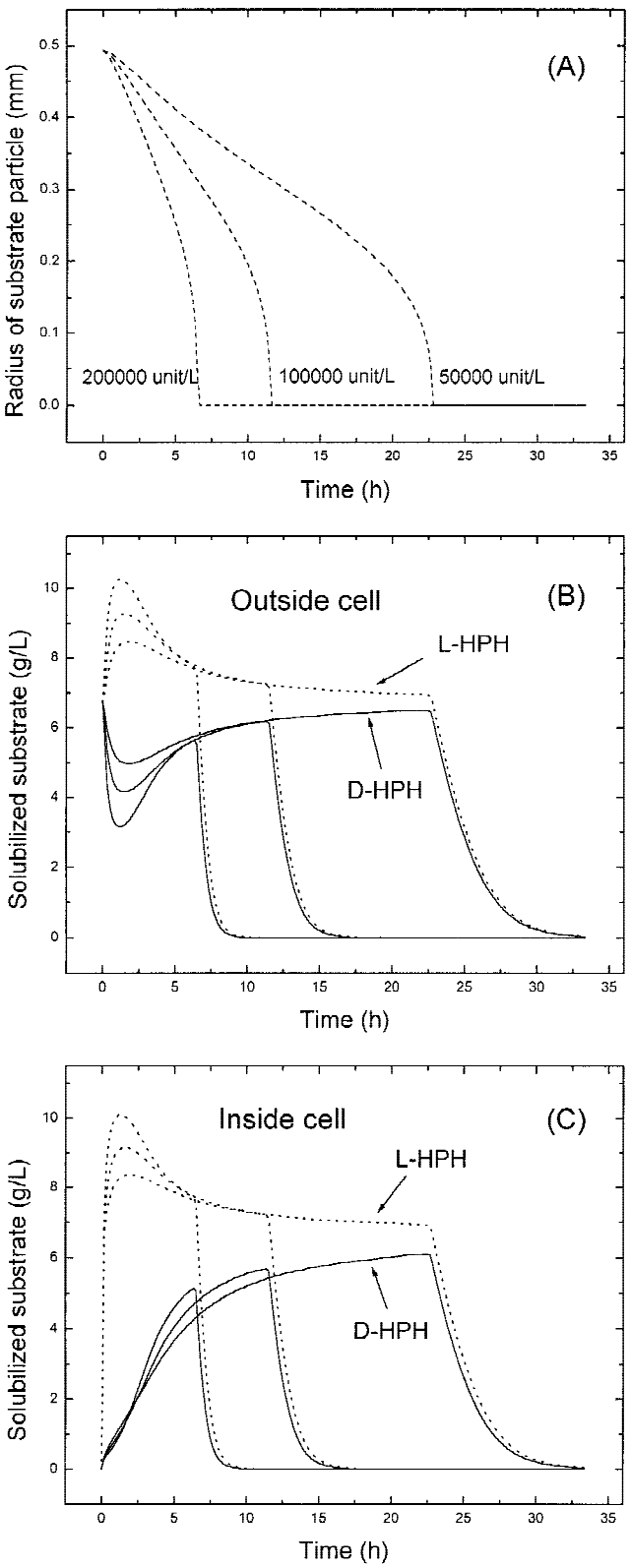

Figure 10. Predicted change in the size of the substrate particles (A), the concentrations of the dissolved D- and L-form substrates in aqueous phase (B), and those inside the cells (C) for the reaction using whole cell enzyme.

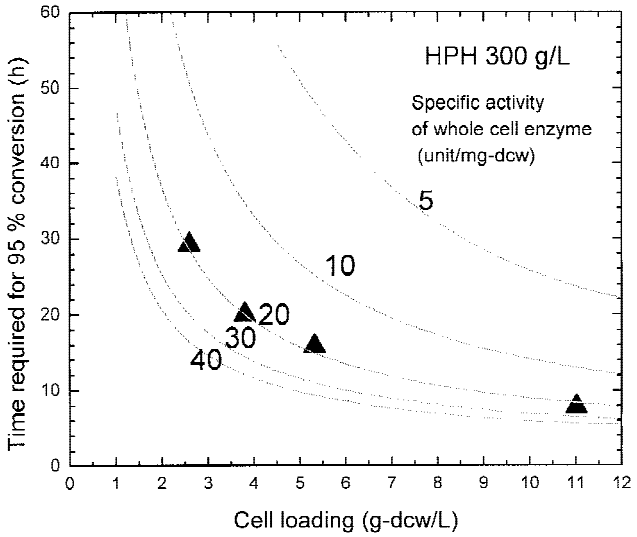

Figure 11. Time required for 95% conversion at different loadings of whole cells when the specific activity of the whole cell enzyme changes. Symbols indicate the experimental results, and solid lines indicate simulation data.

added for titration is dominant, and this deactivation becomes more serious as the enzyme loading increases. Previous observation revealed that high enzyme loading leads to more rapid deactivation of the enzyme (Lee and Kim, 1998), which supports the simulation result. Deactivation of the enzyme by substrate particles increases as the substrate concentration increases. Spontaneous deactivation of the enzyme is assumed to be similar regardless of the reaction conditions. But, portion of spontaneous deactivation is simulated to be high when both the enzyme loading and the substrate concentration are low, and this can be explained by the fact that the relative portion of spontaneous deactivation in the total deactivation is different, depending on the reaction conditions.

From the experimental result shown in Fig. 4, it was observed that when the enzyme loading was lower than a certain level, for example 47,000 and 70,000 units/L, the maximum conversion was not obtained even for a prolonged reaction time. This might be attributed to complete deactivation of the enzyme as shown by simulation. When the enzyme loading is 105,000 units/L, the residual activity drops below 10% of initial value at 5 h reaction.

Simulation of Whole Cell Enzyme System

Profiles of product formation using whole cell enzyme were also simulated. Predicted product concentration represents the sum of each concentration both in cells and in the aqueous phase. As shown in Fig. 7, the experimental results coincided well with the simulation ones for different reaction conditions. At the beginning of the reaction, the production rate was relatively low compared with that of free enzyme, resulting in a sigmoid shape in the production profile, and this can be explained in terms of the permeability of the substrate through the cell membrane (Fig. 7A). In the model for the whole cell enzyme system, the transport barrier for substrate and product through the cell membrane is taken into account. Based on the experimental observation shown in Fig. 3, a saturation kinetic was employed to describe the change in the permeability of the dissolved substrate and product through the cell membrane. In the determination of the kinetic parameters by using nonlinear regression analysis, the P_m value, which indicates the time required to reach half the maximum permeability, was estimated to be different, depending on the substrate concentration; for 50 g/L substrate, P_m was 5.7 h, and for 300 g/L substrate, P_m was 1.1 h. Accordingly, the time course of the change in the permeability is expected to vary with substrate concentration. As shown in Fig. 8, permeability of the substrate through the cell membrane increases more rapidly at 300 g/L substrate than at 50 g/L. The time required for the whole cells to be fully permeabilized was observed to shorten with increasing substrate concentration in our previous work (Lee and Kim, 1998), which supports the simulation result.

Deactivation of the whole cell enzyme in the heterogeneous reaction system also was predicted with reaction time (Fig. 9). Since the enzymes are present inside the cell membrane, deactivation of the enzyme by the substrate particles was assumed to be negligible. Deactivation of the enzyme by NaOH added for titration was predicted to be dominant as in the free enzyme system, but the residual activity of the whole cell enzyme is much higher than that of the free enzyme. As can be seen in Fig. 7, the conversion reached a maximum value even at a lower loading of the whole cell enzyme, and this might be attributed to the fact that the whole cell enzyme is less deactivated than the free enzyme in the heterogenous reaction system.

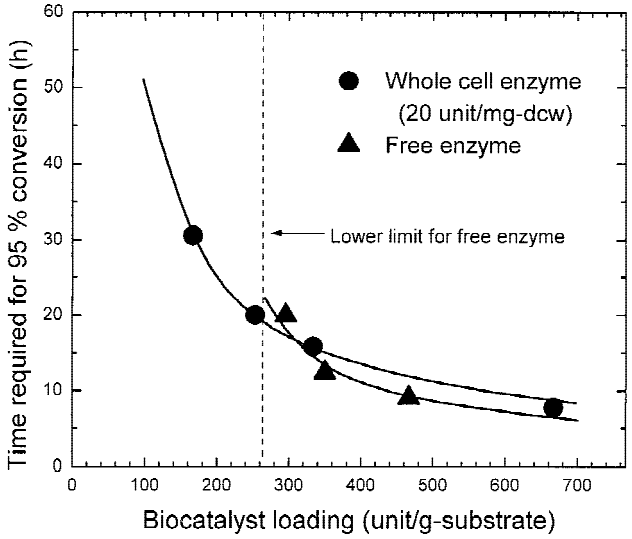

Figure 12. Comparison of the time required for 95% conversion between free and whole cell enzymes at different biocatalyst loadings. Symbols indicate the experimental data, and solid lines simulation ones. Specific activity of the whole cell enzyme was 20 units/mg-dry cell weight.

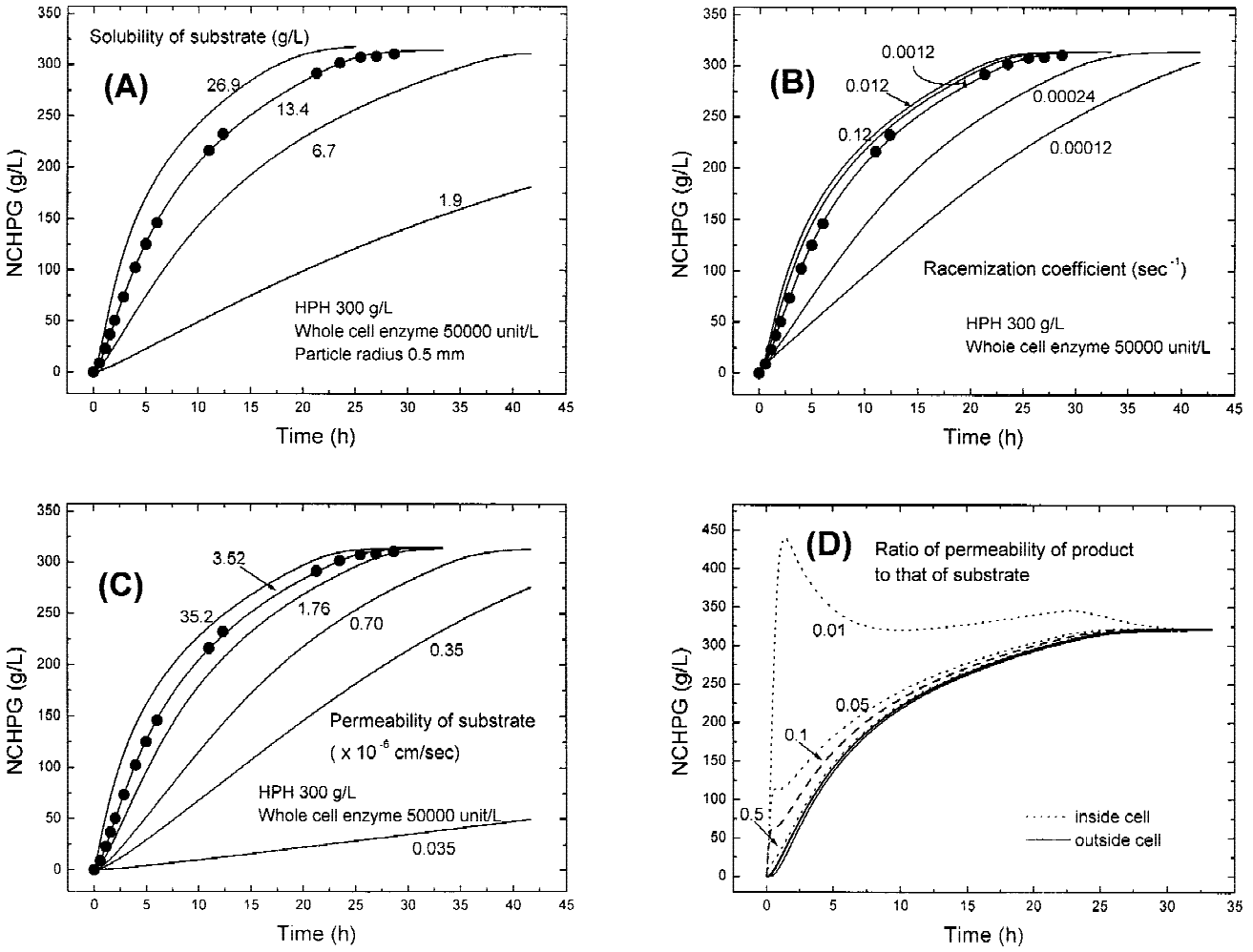

Figure 13. Effect of kinetic parameter values on the profiles of product formation: (A) solubility of substrate, (B) the racemization rate between the dissolved D- and L-form substrates, (C) the maximum permeability of substrate across the cell membrane, and (D) maximum permeability of product through the cell membrane.

Change in the particle size is predicted in Fig. 10A, and a similar pattern is obtained to that for the free enzyme system. Profiles of the dissolved substrate concentration inside and outside the cells are shown in Fig. 10B and C. Concentration of the D-form substrate inside cells is mainly affected by the transfer rate of the dissolved substrate into the cells and the enzyme reaction rate. At the beginning of the reaction, the D-form substrate concentration inside cells is very low because the consumption rate by the enzyme is much higher than the transfer rate. As the enzyme reaction proceeds, the D-form substrate concentration inside the cells gradually increases, and this can be explained by the fact that the enzyme reaction rate reduces with reaction time due to deactivation of the enzyme but the transfer rate of the substrate into cells increases by permeabilization of the cell membrane.

Optimal Cell Loading

When the recombinant *E coli* cells as biocatalyst are directly used in the enzymatic reaction system, the specific activity of the whole cell enzyme might be changed with the culture conditions and the expression level. Consequently, the loading of whole cell enzyme to obtain a certain level of conversion in a predetermined reaction time would also be influenced by the specific activity of the whole cell enzyme. Figure 11 shows the effect of the cell loading on the time required for 95% conversion when the specific activity of the whole cell enzyme ranges from 5 to 40 units/mg-DCW. Symbols indicate the experimental data obtained from the reactions using whole cell enzyme with the specific activity of 20 units/mg-DCW, and a good agreement with the simulation results was observed. This plot can be useful for determining the optimal cell loading to obtain 95% conversion in a planned reaction time when the specific activity of the whole cell enzyme is different.

Performance of Free and Whole Cell Enzyme Systems

To compare the performance of the free and whole cell enzymes in the heterogeneous reaction system, the time

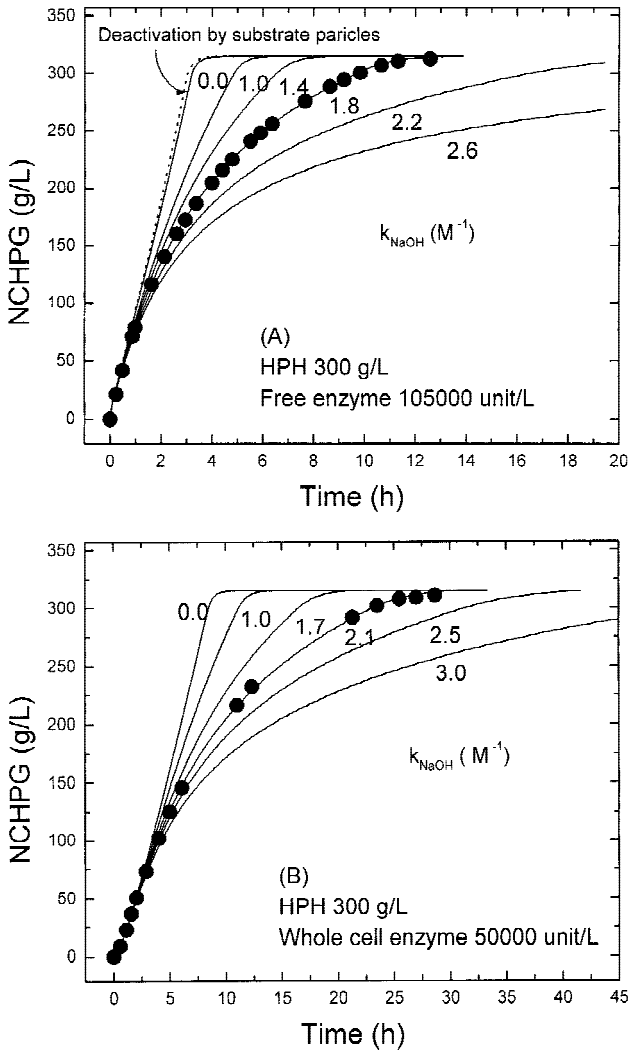

Figure 14. Effect of deactivation constant of enzyme by NaOH on the profiles of product formation: (A) whole cell enzyme and (B) free enzyme.

required for 95% conversion was investigated as a function of biocatalyst loading (Fig. 12). When the free enzyme is used, there exists a certain level of enzyme loading below which the maximum conversion yield is not achieved, and this was found to be due to the complete deactivation of the enzyme. According to the simulation result, at least 260 units/g-substrate is required to obtain 95% conversion. On the other hand, in the case of using whole cell enzyme, the conversion reached the maximum at lower loadings than those of the free enzyme even though the reaction time for 95% conversion is prolonged. There is no significant difference in the reaction time for 95% conversion between free and whole cell enzymes when the biocatalyst loading exceeds about 300 units/g-substrate despite the existence of a transport barrier for substrate and product through the cell membrane. This can be attributed to the permeabilization of the cell membrane during the reaction.

Sensitivity Analyses

In order to evaluate the validity of the kinetic parameters and to investigate the effect of each kinetic parameter on the kinetics of the heterogeneous reaction system, the sensitivity for each parameter was typically examined for the whole cell enzyme system.

Figure 13A shows the effect of the substrate solubility on the profiles of the product formation when the substrate concentration is 300 g/L. Symbols represent the experimental result, and the simulation using the solubility value of 13.4 g/L gives a good agreement. Effect of the racemization coefficient is predicted in Fig. 13B. The racemization coefficient ranging from 0.12 to 0.0012 leads to a small variation in the production profile. It can be seen from Fig. 13A and B that an increase in the substrate solubility and racemization rate can improve the production rate, but not above 20%. The kinetic parameters such as substrate solubility and racemization rate are mainly affected by the pH and temperature of the reaction system. The sensitivity analyses demonstrate that the reaction conditions optimized for the heterogeneous reaction systems in our previous work (Lee and Kim, 1998) are well coincident with those simulated in this work.

Effect of the maximum substrate permeability across the cell membrane was analyzed on the production profile (Fig. 13C). The simulation with the permeability value of 3.62×10^{-6} cm/s gave a good agreement with the experimental result. The production rate seriously declines, as the permeability becomes lower than 0.76×10^{-6} cm/s. Profile of the product concentration inside and outside the cells is shown in Fig. 13D at the different ratios of permeability between product and substrate. When the permeability of product is 2 orders of magnitude lower than that of substrate, the product seriously accumulates inside the cells at the beginning of the reaction, and then gradually decreases due to the permeabilization of the cell membrane. On the other hand, the product concentration outside the cells is not influenced by the ratio of permeability.

Figure 14 shows the effect of enzyme deactivation by NaOH on the reaction performance, and that small change in the k_{NaOH} results in a large variation in the profiles of product formation, confirming that the kinetics of the reaction system is most significantly affected by the k_{NaOH} value. Given that there exists only a spontaneous deactivation of enzyme, the product formation profile would increase linearly with reaction time. Thus, decrease in the production rate with increasing reaction time seems to be mainly due to the deactivation of enzyme by NaOH solution added for titration.

CONCLUSION

The kinetic model developed here well described the heterogeneous reaction system consisting of poorly soluble substrate suspension for the production of optically active D-amino acid using isolated or whole cell D-hydantoinase. The model involved dissolution of solid substrate, enzymatic reaction, spontaneous racemization of L-form substrate to D-form, and deactivation of enzymes. Simulation of the model and sensitivity analyses of the kinetic parameters confirmed the validity of the model. From the simulation

results, it was revealed that deactivation of the enzyme by NaOH added for titration affects most significantly the kinetics of the heterogeneous reaction system. Whole cell enzyme was predicted to be more effective in the reaction system in terms of conversion yield. The presented kinetic model might find application to the optimization of a heterogeneous reaction system for enzymatic conversion of other poorly soluble substrates and to the prediction of their performance using a proper biocatalyst.

Nomenclature

S	concentration of HPH in the aqueous phase (mol/L)
S^*	saturated concentration of HPH in water (mol/L)
S_D	concentration of D-HPH in aqueous phase (mol/L)
S_L	concentration of L-HPH in aqueous phase (mol/L)
$S_{D,C}$	concentration of D-HPH inside cells (mol/L)
$S_{L,C}$	concentration of L-HPH inside cells (mol/L)
P	concentration of NCHPG in aqueous phase (mol/L)
P_C	concentration of NCHPG inside cells (mol/L)
E	concentration of active enzyme in aqueous phase (mol/L)
E_C	concentration of active enzyme inside cells (mol/L)
R_0	initial radius of substrate particle (m)
R	radius of substrate particle during reaction (m)
N_p	number of substrate particles in aqueous phase (m^{-3})
V_{aq}	volume of aqueous phase (m^3)
V_C	total cell volume (m^3)
A_C	surface area of cells per unit volume of aqueous phase (m^{-1})
k_s	mass transfer coefficient (m/s)
k_R	racemization rate constant (s^{-1})
k_{cat}	catalytic constant of enzyme for D-HPH (s^{-1})
K_m	Michaelis–Menten constant of the enzyme for D-HPH (mol/L)
k_d	deactivation constant of the enzyme (s^{-1})
$k_{d,aq}$	constant for spontaneous deactivation of the enzyme in aqueous phase (s^{-1})
$k_{d,C}$	constant for spontaneous deactivation of the enzyme inside cells (s^{-1})
k_p	deactivation constant of free enzyme by solid substrate particles (m/s)
$k_{NaOH,aq}$	deactivation constant of free enzyme by NaOH solution added for titration [$(mol/L)^{-1}$]
$k_{NaOH,C}$	deactivation constant of whole cell enzyme by NaOH solution added for titration [$(mole/L)^{-1}$]
h_S	permeability of HPH across cell membrane (m/s)
$h_{S,0}$	permeability of HPH across cell membrane at time zero (m/s)
$h_{S,max}$	maximum permeability of HPH across cell membrane (m/s)
h_P	permeability of NCHPG across cell membrane (m/s)
P_m	time required to reach half the $h_{S,max}$ (s)
α	ratio of h_P to h_S (—)
C_{NaOH}	concentration of NaOH solution added for titration (mol/L)
a_P	specific surface area of substrate particles (m^{-1})
ρ_H	molar density of HPH particle (mol/L)

REFERENCES

Cecere F. 1975. Substrate and steric specificity of hydropyrimidine hydrase. FEBS Lett 57:192–194.

Constantinides A. 1980. Steroid transformation at high substrate concentration using immobilized *Corynebacterium simplex* cells. Biotechnol Bioeng 22:119–136.

Constantinides A. 1987. Applied numerical methods with personal computers. New York: McGraw-Hill, Inc.

Deepa S, Sivasankar B, Jayaraman K, Prabhakaran K, George S, Palani P. 1993. Enzymatic production and isolation of D-amino acids from the corresponding 5-substituted hydantoins. Process Biochem 28: 447–452.

Jadhav SV, Pangarkar VG. 1991. Particle–liquid mass transfer in mechanically agitated contactors. Ind Eng Chem Res 30:2496–2503.

Johnson ML, Faunt LM. 1992. Parameter estimation by least-squares methods. In: Brand L, Johnson ML, editors. Methods in Enzymology. San Diego: Academic Press, Inc. Vol. 210, p 1–36.

Lee CK, Lin KC. 1996. N-Carbamoyl-D-p-hydroxyphenylglycine production using immobilized D-hydantoinase from recombinant *E. coli.* Enzyme Microb Technol 19:623–627.

Lee DC, Kim GJ, Cha YK, Lee CY, Kim HS. 1997. Mass production of thermostable D-hydantoinase by batch culture of recombinant *Escherichia coli* with a constitutive expression system. Biotechnol Bioeng 56:449–455.

Lee DC, Kim HS. 1998. Optimization of a heterogeneous reaction system for the production of optically active D-amino acid using thermostable D-hydantoinase. Biotechnol Bioeng 60:729–738.

Lee DC, Lee SG, Hong SP, Sung MH, Kim HS. 1996. Cloning and overexpression of thermostable D-hydantoinase from thermophile in *E. coli* and its application to the synthesis of optically active D-amino acids. Ann NY Acad Sci 799:401–405.

Lee SG, Lee DC, Hong SP, Sung MH, Kim HS. 1995. Thermostable D-hydantoinase from thermophilic *Bacillus stearothermophilus* SD-1: Characteristics of purified enzyme. Appl Microbiol Biotechnol 43: 270–276.

Mall S, Buckton G, Gregori T, Rawlins DA. 1995. Investigation of a relationship between surface energy terms and the thermodynamics of transfer of drugs into sodium dodecyl sulfate micelles. J Phys Chem 99:8356–8361.

Maxon WD, Chen JW, Hanson FR. 1966. Simulation of a steroid bioconversion with a mathematical model. Ind Eng Chem Process Design Dev 5:285–289.

Ogawa J, Chung M, Hida S, Yamada H, Shimizu S. 1994. Thermostable N-carbamoyl-D-amino acid amidohydrolase: Screening, purification, and characterization. J Biotechnol 38:11–19.

Olivieri R, Fascetti E, Angelini L, Degen L. 1981. Microbial transformation of racemic hydantoins to D-amino acids. Biotechnol Bioeng 23: 2173–2183.

Runser S, Chinski N, Ohleyer E. 1990. D-p-Hydroxyphenylglycine production from D,L-5-p-hydroxyphenylhydantoin by *Agrobacterium* sp. Appl Microbiol Biotechnol 33:382–388.

Shugar GJ, Ballinger JT. 1996. Chemical technicians' ready reference handbook. 4th ed. New York: McGraw-Hill, Inc.

Singleton P, Sainsbury D. 1987. Dictionary of microbiology and molecular biology. 2nd ed. New York: Wiley-Interscience.

Syldatk C, Läufer A, Müller R, Höke H. 1990. Production of optically pure D- and L-α-amino acids by bioconversion of D,L-5-monosubstituted hydantoin derivatives. Adv Biochem Eng/Biotechnol 41:29–75.

Takahashi S. 1986. Microbial production of D-p-hydroxyphenylglycine. Prog Ind Microbiol 24:269–279.

Tranchino L, Melle F. 1990. Modeling and control of the biocatalytic conversion of hydantoins to D-amino acids. Ann NY Acad Sci 589: 553–568.

Wolff A, Zhu L, Kielland V, Straathof JJ, Jongejan JA, Heijnen JJ 1997. Simple dissolution–reaction model for enzymatic conversion of suspension of solid substrate. Biotechnol Bioeng 56:433–440.

Yamada H, Takahashi S, Kii Y, Kumagai H. 1978. Distribution of hydantoin hydrolyzing activity in microorganisms. J Ferment Technol 56: 484–491.